Characterization of SPAK and OSR1, Regulatory Kinases of the Na-K-2Cl Cotransporter

Kenneth B. E. Gagnon, Roger England, and Eric Delpire*

Department of Anesthesiology, Vanderbilt University Medical Center, Nashville, Tennessee 37232

Our recent studies demonstrate that SPAK (*Ste20p-related Proline Alanine-rich Kinase*), in combination with WNK4 [*With No lysine (K) kinase*], phosphorylates and stimulates the Na-K-2Cl cotransporter (NKCC1), whereas catalytically inactive SPAK (K104R) fails to activate the cotransporter. The catalytic domain of SPAK contains an activation loop between the well-conserved DFG and APE motifs. We speculated that four threonine residues (T231, T236, T243, and T247) in the activation loop might be sites of phosphorylation and kinase activation; therefore, we mutated each residue into an alanine. In this report, we demonstrate that coexpression of SPAK (T243A) or SPAK (T247A) with WNK4 not only prevented, but robustly inhibited, cotransporter activity in NKCC1-injected *Xenopus laevis* oocytes. These activation loop mutations produced an effect similar to that of the SPAK (K104R) mutant. In vitro phosphorylation experiments demonstrate that both intramolecular autophosphorylation of SPAK and phosphorylation of NKCC1 are significantly stronger in the presence of Mn^{2+} rather than Mg^{2+}. We also show that SPAK activity is markedly inhibited by staurosporine and K252a, partially inhibited by *N*-ethylmaleimide and diamide, and unaffected by arsenite. OSR1, a kinase closely related to SPAK, exhibited similar kinase properties and similar functional activation of NKCC1 when coexpressed with WNK4.

Cation-chloride cotransporters (e.g., Na-K-2Cl and K-Cl cotransporters) serve multiple fundamental functions in a wide variety of tissues and organs. These include influencing ion and fluid movements in secreting or reabsorbing epithelia, control of CNS excitability, and cell volume regulation, proliferation, and survival (for a review, see reference 19). On the basis of the observations that the cotransporters are phosphoproteins and that phosphatase inhibitors affect cotransport activity, it is generally agreed that cotransporter regulation is mainly mediated through phosphorylation-dephosphorylation mechanisms. Activity of NKCC1, for instance, correlates directly with the phosphorylation state of the protein (33). For the past 20 years, the identity of the kinase in question has remained elusive. We have recently shown direct interaction between cation-chloride cotransporter and two Ste20p-related serine/threonine kinases, SPAK and OSR1 (45).

There are some 30 protein kinases identified in mammals related to the budding *Saccharomyces cerevisiae* sterile 20 protein kinase (Ste20p). In 1991, Dan et al. divided the mammalian Ste20p-like kinases into two subgroups: the p21-activated kinases (PAKs; two subfamilies), which are characterized by a carboxyl-terminal catalytic domain, and the germinal center kinases (GCKs; eight subfamilies), which have their catalytic domain located at the amino terminus (10). Most Ste20p-like kinases stimulate mitogen-activated protein kinase (MAPK) cascades and thus participate in the modulation of cell motility (7), cell growth (31), and apoptosis (23).

The GCK6 subfamily comprises two kinases: SPAK/PASK (Ste20-related proline alanine-rich kinase) (26, 52) and OSR1 (oxidative stress response 1) (50). These two closely related kinases share 66% identity overall at the amino acid level, are structurally reminiscent of MST kinases, and possess a well-conserved, short, and unique C-terminal region. This unique region was demonstrated to be a critical domain of the kinase, interacting with RFxV motifs in membrane transport systems such as cation-chloride cotransporters (45) and chloride channels (12) but also associating with other proteins such as heat shock protein 105, WNK4, apoptosis-associated tyrosine kinase, gelsolin (44), the actin cytoskeleton (51), and p38 MAPK (26, 44).

Functionally, SPAK increases the activity of the Na-K-2Cl cotransporter (13, 18), reduces the activity of the neuron-specific K-Cl cotransporter, KCC2 (18), and inactivates the cell cycle-dependent CLC anion channel in *Caenorhabditis elegans* (12). Consistent with their role in ion transport, SPAK and OSR1 expression increases in killifish opercular epithelium as the fish adapts from seawater to fresh water (35). Thus, modulation of ion transport seems to be a major function of the kinase and, not surprisingly, the highest levels of kinase expression are seen in the secretory cell in *C. elegans* (12) and in mouse secreting and absorbing epithelia (36, 45, 52). However, OSR1 and SPAK have also been shown to carry out additional functions, such as acting as intermediates in cell signaling. For example, increasing concentrations of sorbitol activate OSR1, which phosphorylates the N-terminal regulatory domain of PAK1, desensitizing the kinase to activation by small G proteins (8). In 2004, Li et al. (30) found that SPAK serves as an intermediate in a T-cell-receptor-induced signaling pathway. Activation of the transcription factor AP-1 requires protein kinase C-θ (PKCθ) phosphorylation of two specific SPAK serine residues: S311 and S325. We recently demonstrated that SPAK activation of NKCC1 and deactivation of KCC2 in *Xenopus laevis* oocytes requires a functional interaction with an-

---

* Corresponding author. Mailing address: Department of Anesthesiology, Vanderbilt University Medical Center, T-4202 Medical Center North, 1161 21st Avenue South, Nashville, TN 37232. Phone: (615) 343-7409. Fax: (615) 343-3916. E-mail: eric.delpire@vanderbilt.edu.

other upstream kinase: WNK4 (18). Vitari and coworkers confirmed this interaction between SPAK, WNK1, and WNK4 (54). They also showed that the two WNK kinases phosphorylate SPAK at residue T243 in the activation loop and at residue S383 in the regulatory subdomain (mouse sequence). Thus, SPAK is a target for at least three upstream kinases: PKCθ, WNK4, and WNK1. Furthermore, there seems to be some specificity to the residues phosphorylated by these upstream kinases.

Through in vitro phosphorylation studies, we examined the modalities of mouse SPAK and OSR1 autophosphorylation and transphosphorylation of the N-terminal tail of NKCC1. We show that the in vitro activity of both SPAK and OSR1 is stronger in the presence of Mn^{2+} rather than Mg^{2+} and that both have high affinities for ATP and are inhibited by high Cl^- concentrations. We demonstrate that autophosphorylation occurs through intramolecular rather than intermolecular reactions and that two of the four threonine residues located in the activation loop of the kinase (T243 and T247) are critical for SPAK activity in vitro as well as in vivo activation of NKCC1 in *Xenopus laevis* oocytes.

MATERIALS AND METHODS

Mutagenesis of SPAK. A 800-bp AflII-BglII fragment from mouse SPAK cDNA containing the "activation loop" between the DFG and APE motifs was PCR amplified and subcloned into pGEM-T Easy vector (Invitrogen, Carlsbad, CA). Complementary sense and antisense oligonucleotides containing the codon GCN (Ala) instead of ACN (Thr) were used to individually mutate the four threonine residues into alanines (QuikChange; Stratagene, La Jolla, CA). The parental DNA was digested with DpnI to cleave methylated GATC sequences, and a 1-μl aliquot of the PCR was transformed into *Escherichia coli*. Several clones were isolated to verify proper sequence and mutation. The AflII-BglII fragment was then reinserted into the original SPAK clone in pGEX. Each of the four Thr→Ala mutant SPAK clones were also moved to the *Xenopus* expression vector pBF with EcoRI-XhoI. Two PCRs using nested sense and antisense oligonucleotides were used to excise the proline- and alanine-rich region (PAPA box) located upstream of the catalytic domain of SPAK. The sequence of the final PCR product was verified, and the EcoRI-EcoRV fragment was reinserted into the original SPAK clone in pGEX and pBF vectors. A SacI fragment from the full-length catalytically inactive SPAK was then moved to the shortened SPAK (-PAPA box) clone to create a smaller, catalytically inactive SPAK.

Cloning of mouse OSR1. We obtained IMAGE clone 5341146 (mouse OSR1) from ATCC, subcloned it into pBluescript vector (pBSK+), and sequenced the entire insert. A SacI-BamHI fragment was PCR amplified from mouse brain, sequenced, and then substituted into the original clone to correct for an insertion. Adaptors made of complementary oligonucleotides (KpnI-XhoI at the 5′ end and BstXI-NotI at the 3′ end) were used to remove both 5′ and 3′ untranslated regions. The full-length mouse OSR1 clone was then moved into pBF and pGEX vectors.

GST fusion protein production. Wild-type and mutant SPAK, OSR1, and NKCC1 constructs in pGEX were transformed into protease-deficient *E. coli* cells and incubated at 30°C for 3 to 4 h until reaching an optical density at 600 nm > 0.5. Fusion protein production was then induced by the addition of 24 mg/liter IPTG (isopropyl-β-D-thiogalactopyranoside) for an additional 4 h, and then the cells were collected by centrifugation at 4°C, resuspended in column buffer (140 mM NaCl, 2.7 mM KCl, 10 mM Na_2HPO_4, 1.8 mM KH_2PO_4) containing protease inhibitors, and frozen at −20°C. *E. coli* cells were lysed by sonication, incubated with Triton X-100 (1% final) for 30 min on ice, and spun down at 10,000 × g for 10 min at 4°C. The supernatant was passed through a column containing glutathione-Sepharose beads, and the fusion protein-bead complex was washed overnight with phosphate-buffered saline at 4°C. Bacterial chaperone proteins attached to misfolded glutathione *S*-transferase (GST) fusion proteins were removed using a 10 mM Mg-ATP wash (according to the Pharmacia manual instructions). Fusion proteins were eluted using 10 mM glutathione in 50 mM HEPES and concentrated using a 30-kDa cutoff Amicon ultra spin filter.

In vitro kinase assays. Kinase reactions with each of the GST fusion proteins were carried out using a 30-μl volume containing 20 mM HEPES (pH 7.4), 2 mM $MnCl_2$, 5 mM dithiothreitol (DTT), 2 μM cold ATP, and 8 μCi [γ-^{32}P]ATP at 37°C for 45 min. Reactions were stopped by adding 30 μl of 2× sodium dodecyl sulfate (SDS) sample buffer followed by denaturing at 70°C for 15 min. Reaction products were separated by SDS-polyacrylamide gel electrophoresis (PAGE) on a 10% polyacrylamide gel. Gels were washed three times for 10 min each in a buffer containing 1% sodium pyrophosphate and 5% trichloroacetic acid and dried at 60°C for 2 h, and phosphorylated products were visualized by autoradiography.

Western blot analysis. GST-SPAK fusion proteins (~5 μg) were resolved by SDS–10% PAGE and electroblotted onto polyvinylidene difluoride membranes. Membranes were blocked for 2 h at room temperature with 5% nonfat dry milk in TBST (150 mM NaCl, 10 mM Tris-HCl, 0.5% Tween 20 [polyoxyethylene-sorbitan monolaurate]) and then incubated overnight at 4°C with either a polyclonal N-terminal or C-terminal anti-SPAK antibody (1:1,000) in TBST–5% nonfat dry milk. Membranes were washed extensively in TBST, and protein bands were visualized by enhanced chemiluminescence (ECL Plus; Amersham Biosciences, Piscataway, NJ).

cRNA synthesis. All cDNA clones in pBF were linearized with MluI and transcribed into cRNA by use of Ambion's mMESSAGE mMACHINE SP6 transcription system (Ambion, Austin, TX). RNA quality was verified by gel electrophoresis (1% agarose–0.693% formaldehyde), and RNA was quantitated by measurement of absorbance at 260 nm.

Isolation of *Xenopus laevis* oocytes. Stage V to VI *Xenopus laevis* oocytes were isolated from eight different frogs as previously described (44, 49) and maintained at 16°C in modified L15 medium (Leibovitz's L15 solution diluted with water to a final osmolarity of 195 to 200 mosM and supplemented with 10 mM HEPES and 44 μg gentamicin sulfate). Oocytes were injected on day 2 with 50 nl water containing 15 ng NKCC1 cRNA and on day 3 with 50 nl water containing 10 ng of each kinase cRNA. Control oocytes were injected with 50 nl water. ^{86}Rb uptake determinations were performed on day 5 postisolation.

K$^+$ uptakes in *Xenopus laevis* oocytes. Groups of 20 oocytes in a 35-mm dish were washed once with 3 ml isosmotic saline solution (96 mM NaCl, 4 mM KCl, 2 mM $CaCl_2$, 1 mM $MgCl_2$, 5 mM HEPES buffered to pH 7.4) and preincubated for 15 min in 1 ml of the same isosmotic saline solution containing 1 mM ouabain. The solution was then aspirated and replaced with 1 ml isosmotic flux solution containing 5 μCi ^{86}Rb. Two 5 μl aliquots of flux solution were sampled at the beginning of each ^{86}Rb uptake period and used as standards. After 1 h uptake, the radioactive solution was aspirated and the oocytes were washed four times with 3 ml ice-cold isosmotic solution. Single oocytes were transferred into glass vials, lysed for 1 h with 200 μl 0.25N NaOH, and neutralized with 100 μl glacial acetic acid, and ^{86}Rb tracer activity was measured by β-scintillation counting. NKCC1 flux is expressed in nanomoles K$^+$/oocyte/hour.

Yeast two-hybrid analysis. Full-length SPAK and portions of PCR-amplified NKCC1 were inserted in the yeast vector pGBDUc2 and transformed into competent PJ69-4A yeast cells. Yeast cells containing SPAK or NKCC1 were then transformed with either the regulatory domain of SPAK or full-length WNK4 inserted in pACTII. The transformed yeast cells were plated on double dropout (uracil and leucine dropout) plates for measuring transformation efficiency and triple dropout (uracil, leucine, and histidine dropout) plates for determining protein-protein interaction. Yeast survival was assessed after 2 to 4 days at 30°C.

Statistical analyses. Differences between ^{86}Rb uptake groups were tested by one-way analysis of variance followed by multiple comparisons using Student-Newman-Keuls, Bonferroni, and Tukey posttests. $P > 0.001$ was considered to be very significant.

RESULTS

Schematic and structural representation of SPAK. The general features of SPAK and amino acid residues mutated in this study are indicated schematically in Fig. 1A. The kinase contains a short N-terminal sequence rich in proline and alanine residues (PAPA box), located upstream of the catalytic domain. Four threonine residues (T231, T236, T243, and T247) identified in the activation loop are located upstream of a region containing a quartet of highly conserved hydrophobic residues (F244, M251, P253, and L278). The representation also identifies serine residues S321 and S383, which are targets
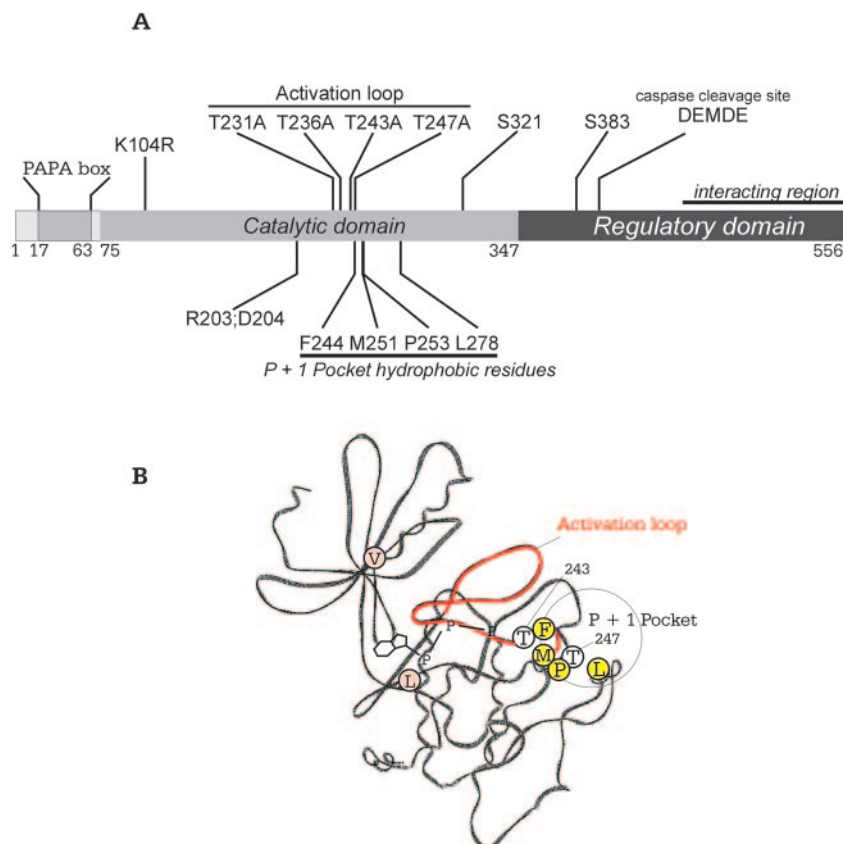
FIG. 1. Schematic and structural representation of SPAK. (A) The catalytic domain of SPAK with the N-terminal PAPA box, activation loop, and P+1 hydrophobic pocket are depicted. A caspase cleavage site and a large protein-protein interaction region within the regulatory domain are also indicated. Specific residues mutated in this study are identified. (B) SWISS-PROTEIN model of the catalytic domain of SPAK highlighting conserved hydrophobic residues (V89, L205) which sandwich the adenosine ring of ATP; the activation loop (red backbone) with residues T243 and T247; and four residues (F244, M251, P253, L278) lining a hydrophobic P+1 pocket for substrate interaction.

of PKCθ and of WNK1 and WNK4, respectively. The C-terminal regulatory domain contains a caspase cleavage site and a relatively large region that interacts with R/KFxV/I motifs in many proteins. A wire-frame representation of the kinase domain of SPAK was constructed by SWISS-MODEL, based on the crystal structures of two Ste20 kinases, PAK1 and TAO2 (Fig. 1B). The model shows the typical propeller-like structure created by β strands I to VII, the two hydrophobic residues valine and leucine that sandwich the adenosine ring of ATP, four hydrophobic residues, and threonines 243 and 247 in the vicinity of the P+1 pocket.

Kinase activity of SPAK. Wild-type and mutant SPAK proteins were all expressed as GST fusion proteins and purified as described in Materials and Methods. After incubation with [γ-^{32}P]ATP, SDS-PAGE, and autoradiography, wild-type SPAK was visible as two major bands at 87 kDa and 70 kDa (Fig. 2A). Mass spectrometry and Western blot analyses (not shown) confirmed that the 87 kDa band represents full-length SPAK, whereas the smaller 70 kDa band represents a truncated N-terminal portion of SPAK. Wild-type SPAK autophosphorylation is substantial in 2 mM MnCl$_2$ but negligible in either 2 or 5 mM MgCl$_2$ (Fig. 2B), indicating a striking (in vitro) divalent cation specificity. Incorporation of ^{32}P is reduced substantially with excess cold ATP but not GTP, dem-

onstrating that GTP cannot be used as a donor source of phosphate (Fig. 2C). We also show that dithiothreitol concentrations greater than 5 mM do not enhance SPAK autophosphorylation (Fig. 2D) and that kinase activity is sensitive to chloride at physiologically relevant concentrations (Fig. 2E). In vitro autophosphorylation of SPAK is time sensitive, with maximal activity observed between 60 and 90 min at 37°C (Fig. 2F), and the K_m of the kinase for ATP is relatively low, ranging from 5 to 10 μM (Fig. 2G).

Mutation of threonine residues within the activation loop of SPAK prevents autophosphorylation. First, we performed sequential mutation of each of the four threonine residues located between the DFG and APE motifs of the activation loop of SPAK. We identified T243 and T247 as the key residues necessary for SPAK autophosphorylation and transphosphorylation of the N terminus of NKCC1 (Fig. 3A). Single-point mutation of each threonine residue into an alanine verified that neither T231A nor T236A interfered with the kinase activity of SPAK. In contrast, we found that T243A significantly reduces both autophosphorylation and transphosphorylation of NKCC and that mutating T247A completely inhibits all ^{32}P incorporation, in similarity to the results seen with the kinase-inactive SPAK (K104R) mutant (Fig. 3A). To test whether the C-terminal regulatory domain of SPAK is involved in auto-
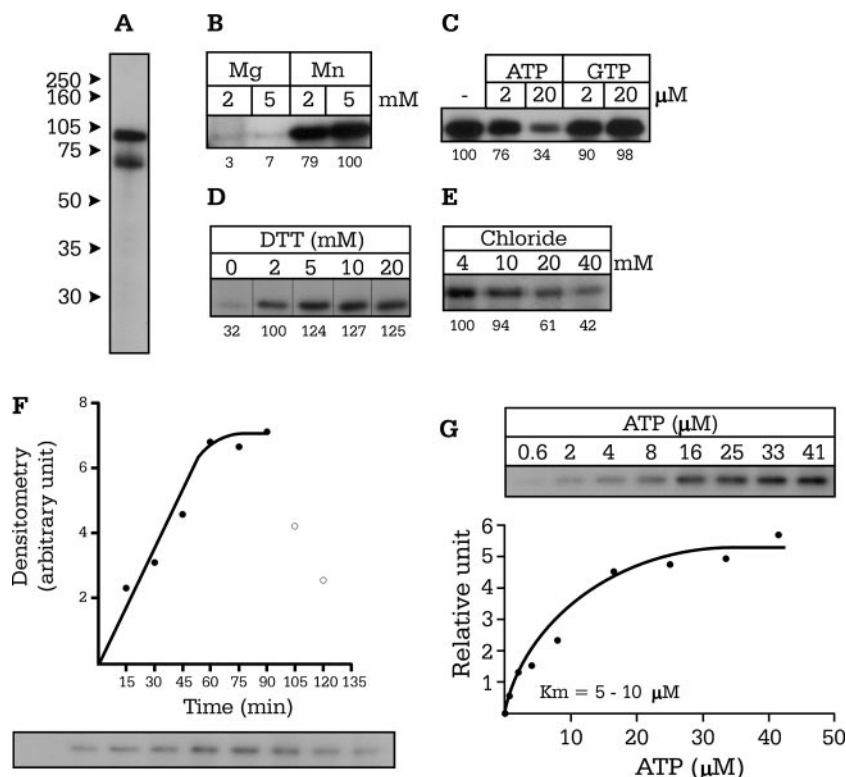
FIG. 2. Optimization of kinase activity of SPAK. (A) Autoradiography of a 10% SDS-PAGE gel showing autophosphorylated SPAK at both 87 and 70 kDa. (B) Autophosphorylation of SPAK in the presence of $MnCl_2$ and $MgCl_2$. (C) Effect of addition of cold Mg-ATP and Mg-GTP on SPAK ^{32}P incorporation. (D to E) Effect of increasing DTT concentrations (1 to 20 mM) and chloride concentrations (4 to 40 mM) on SPAK autophosphorylation. (F) Time course of SPAK autophosphorylation as measured at 37°C. (G) ^{32}P incorporation as a function of ATP concentrations. The K_m values for ATP were measured at 5 μM and 8.3 μM in two separate experiments.

phosphorylation and transphosphorylation of NKCC1, we introduced stop codons at the end of the catalytic domain and within the regulatory domain, before the region of divergence between SPAK and OSR1. We show that removal of the extreme carboxyl tail containing the cotransporter interaction domain (region "f" in Fig. 3B) and the small region of low homology between SPAK and OSR1 (region "e" in Fig. 3B) does not affect SPAK autophosphorylation or SPAK phosphorylation of NKCC1. In contrast, although removal of the entire regulatory domain resulted in the absence of NKCC1 phosphorylation, the kinase was still able to autophosphorylate.

Absence of SPAK-SPAK protein interaction. The Ste20p-like kinase MST1 contains within its regulatory domain a region identified as the site of protein-protein dimerization (21). To assess the presence of such a region in SPAK, we transformed yeast cells with full-length SPAK in pGBDUc2 and the entire regulatory domain of SPAK in pACTII. As indicated in Fig. 4A, there was no yeast survival when full-length SPAK was cotransformed with the regulatory domain of SPAK, whereas there was yeast survival with our positive-control interactions between NKCC1 and the regulatory domain of SPAK and full-length SPAK with full-length WNK4. These data therefore demonstrate the absence of SPAK-SPAK interaction and suggest the absence of a dimerization domain.

Autophosphorylation of SPAK is intramolecular. To determine whether SPAK autophosphorylation occurs within one SPAK molecule (intramolecular reaction) or between separate SPAK molecules (intermolecular reactions), we examined the effect of protein concentration on kinase autophosphorylation. Indeed, if autophosphorylation occurs intermolecularly, as molecules have to interact, incorporation of γ-^{32}P should be dilution dependent. Our data in Fig. 4B and C show a decrease of γ-^{32}P incorporation proportional to protein concentration. Although these data support the idea of an intramolecular autophosphorylation mechanism, the range of protein concentrations was limited by the sensitivity of the kinase assay, leaving the possibility of a dilution effect at lower protein concentrations. Therefore, we used a more direct approach by combining wild-type SPAK with catalytically inactive SPAK (K104R). To clearly identify both proteins on polyacrylamide gel, we shortened the catalytically inactive kinase by removing the PAPA box. When full-length active SPAK was incubated with the shorter inactive SPAK, the active kinase was unable to phosphorylate the inactive kinase, demonstrating that autophosphorylation of SPAK occurs intramolecularly (Fig. 4D). We also shortened the catalytically active kinase to confirm that absence of the PAPA box did not affect SPAK autophosphorylation or transphosphorylation of GST-NKCC1 (Fig. 4D, fourth lane). Furthermore, coexpression of the shortened catalytically active kinase in *Xenopus laevis* oocytes confirmed that the absence of the PAPA box did not affect cotransporter stimulation in the presence of WNK4 (see Fig. 6B).
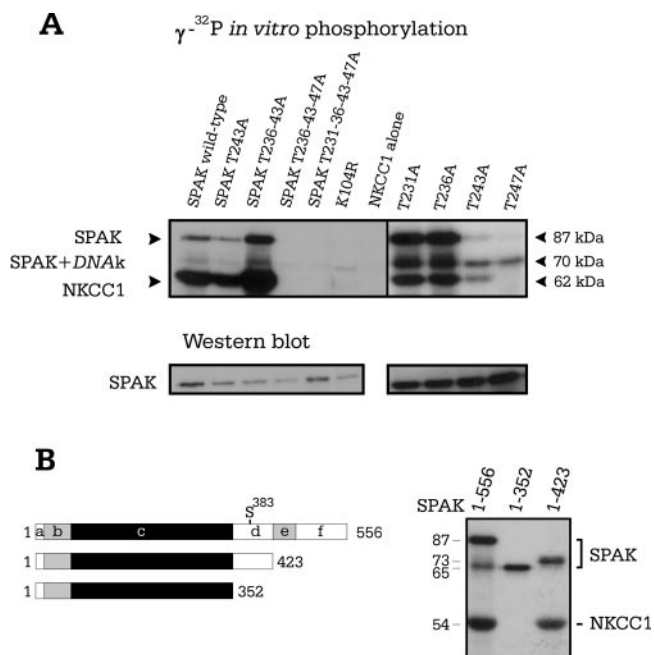
FIG. 3. In vitro phosphorylation studies of SPAK with activation loop and deletion mutants. (A) Wild-type SPAK along with nine mutants was combined with the N-terminal region of NKCC1. To evidence equal protein loading, semiquantitative determination of the 87 kDa SPAK band was obtained using Western blot analysis with a specific N-terminal SPAK antibody. (B) Schematic representation of wild-type and two truncated forms of SPAK. Segment "b" represents the proline-and alanine-rich region (PAPA box), "c" the catalytic domain, "d" the first segment of the C-terminal domain with high homology to OSR1, "e" the region with low homology to OSR1, and "f" the cation-chloride cotransporter interaction domain. The amino acid length of each construct is indicated. The results of an in vitro kinase assay showing autophosphorylation of truncated SPAK mutants and the absence of NKCC1 phosphorylation when segment "d" is missing are shown.

Kinase activity of OSR1. As previously mentioned, OSR1 is the protein most closely related to SPAK, sharing 66% identity at the amino acid level. To determine whether this kinase possesses properties similar to those of SPAK, we performed in vitro phosphorylation experiments using a GST-OSR1 fusion protein and the reaction conditions already established for SPAK (Fig. 5A). In similarity to SPAK results, OSR1 autophosphorylation was substantial in 2 and 5 mM $MnCl_2$ and negligible in either 2 or 5 mM $MgCl_2$ (Fig. 5B) and displayed some sensitivity to high concentrations of chloride (Fig. 5C). We determined the K_m for ATP to be around 1 μM (Fig. 5D).

Activation of NKCC1 by the SPAK-WNK4 complex requires SPAK activation loop threonine phosphorylation. In a previous report, we demonstrated isotonic activation of NKCC1 by coexpressing SPAK and WNK4 in NKCC1-injected *Xenopus laevis* oocytes (18). In the next set of experiments, we tested whether mutation of any of the threonine residues within the activation loop (T231A, T236A, T243A, and T247A) affected the capacity of SPAK to activate the cotransporter. We show that coexpression of WNK4 with either SPAK (T231A) or SPAK (T236A) does not significantly affect the stimulation of cotransporter activity (Fig. 6). However, coexpression of WNK4 with SPAK (T243A) or SPAK (T247A) in NKCC1-

injected *Xenopus laevis* oocytes completely inhibits NKCC1 activity, consistent with an absence of in vitro ^{32}P incorporation (Fig. 3A).

Activation of NKCC1 by OSR1-WNK4. Consistent with the in vitro phosphorylation of NKCC1 by OSR1, coexpression of OSR1 together with WNK4 in *Xenopus laevis* oocytes results in a significant stimulation of cotransporter activity (Fig. 6), reminiscent of the stimulation observed with SPAK. Expression of OSR1 alone in NKCC1-injected oocytes did not stimulate cotransporter activity above basal levels (data not shown).

Inhibitors and activators of cation-chloride cotransporters. Staurosporine and K252A have been shown to reduce NKCC1 activity and to prevent NKCC1 activation in a variety of cells (17, 33, 37, 40, 42). To determine whether these inhibitors exert their influence on the cotransporter by modulating SPAK activity, we examined SPAK autophosphorylation and transphosphorylation of the N-terminal tail of NKCC1 in the presence of 0.1 μM to 100 μM staurosporine and K252a. As shown in Fig. 7, ^{32}P incorporation decreased with increasing concentrations of both kinase inhibitors. Note that the concentration required for half activity ranges from 0.1 to 1 μM for staurosporine and 1 to 10 μM for K252a. *N*-Ethylmaleimide (NEM) markedly activates the activity of K-Cl cotransport (29) while inactivating the Na-K-2Cl cotransporter (37). Although NEM is a rather nonspecific sufhydral reagent, its effect on cation-chloride cotransporter activity likely results from protein kinase inhibition (9, 34). We tested the effect of NEM, and the sulfhydral oxidant diamide, on SPAK activity also using in vitro phosphorylation experiments. As shown in Fig. 7, the two thiol-reacting compounds had minimal impact on SPAK autophosphorylation. However, at concentrations higher than 100 μM, NEM and diamide decreased SPAK phosphorylation of NKCC1. In ferret red cells, arsenite has been shown to cause marked stimulation of Na-K-2Cl cotransport (17), potentially linking cotransporter activation to the involvement of stress-activated protein kinases (27). We examined the role of arsenite on SPAK autophosphorylation and SPAK phosphorylation of NKCC1 and found no effect in the range of 1 to 1,000 μM. Finally, we show that H_2O_2, a strongly oxidizing reagent, reduces SPAK autophosphorylation and SPAK phosphorylation of the N-terminal tail of NKCC1 in the mM range (0.03% [wt/wt] or ~9 mM).

DISCUSSION

We have recently shown that SPAK and OSR1, two Ste20p-like serine-threonine kinases, interact with cation-chloride cotransporters, including the Na-K-2Cl cotransporter, NKCC1 (45). We later showed that WNK4, a kinase involved in pseudohypoaldosteronism (55), also interacts with SPAK through a RFQV binding motif (44) and that this interaction between the two kinases results in significant activation of NKCC1 under isosmotic conditions (18). Because the catalytic activity of both kinases is required for NKCC1 activation and because, in contrast to SPAK, WNK4 failed to interact directly with the cotransporter, we proposed a hierarchy of events in which WNK4 activates SPAK, which in turn phosphorylates NKCC1 (18). Consistent with this idea, Vitari and coworkers have recently presented direct evidence that WNK1 and WNK4 phosphorylate and activate SPAK and OSR1 (54).
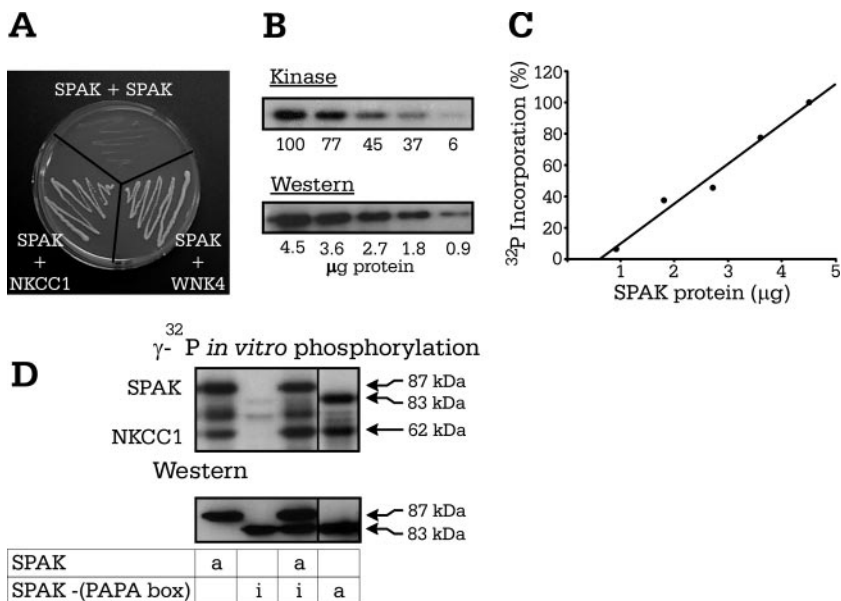
FIG. 4. Autophosphorylation of SPAK is intramolecular. (A) Yeast two-hybrid analysis of SPAK-SPAK interaction showing no yeast survival. Positive controls are SPAK-NKCC1 and SPAK-WNK4 interactions. (B) Level of ^{32}P incorporation of SPAK decreases (upper panel) with the amount of protein present, as determined by Western blot analysis (lower panel). (C) Linear relationship between ^{32}P incorporation and protein concentration as determined by a Bradford assay. (D) In vitro phosphorylation experiment mixing active and inactive forms of SPAK. Western blot analysis using a C-terminal SPAK antibody confirmed the presence of each of the SPAK proteins. Active (wild-type) or inactive (nonfunctional K104R mutant) forms of SPAK are indicated by the letters "a" and "i," respectively.

Activation of many protein kinases requires phosphorylation of the activation segment or loop between two highly conserved tripeptide motifs (DFG. . . .APE) (38). Crystallographic models of phosphorylated and nonphosphorylated protein kinases have demonstrated large movements in their activation loop, allowing better substrate access to the active site, suggesting that the activation loop may function as a "door" to the substrate pocket (25). On the basis of the high degree of conservation between SPAK and this particular group of protein kinases, we speculated that phosphorylation of threonine residues located in the activation loop might be critical in the activation of the kinase. Our experiments show that mutating
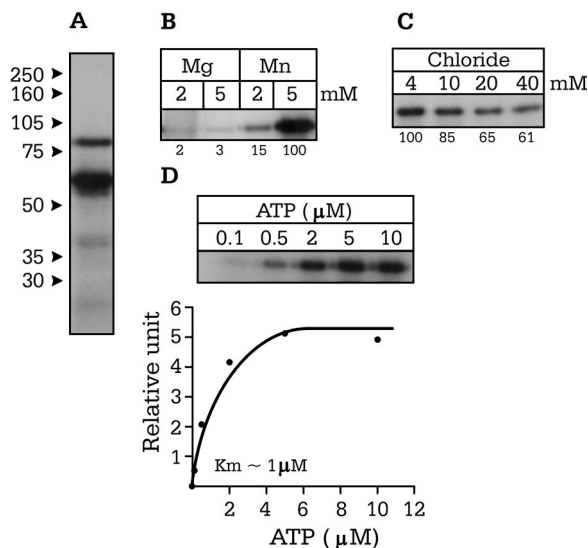

FIG. 5. Characterization of OSR1 kinase activity. (A) Presence of autophosphorylated OSR1 at 77 and 60 kDa. (B) OSR1 autophosphorylation in the presence 2 and 5 mM $MnCl_2$ and $MgCl_2$. (C) Effect of increasing Cl^- concentrations (4 to 40 mM) on ^{32}P incorporation by the kinase. (D) OSR1 autophosphorylation as a function of ATP concentration. The K_m was measured at ~1 μM.
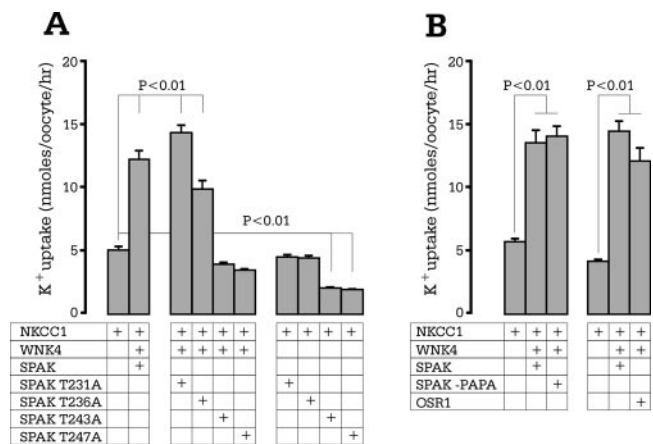

FIG. 6. NKCC1 function requires SPAK activation via loop threonine phosphorylation. (A) Functional analysis of SPAK mutants through ^{86}Rb uptake in Xenopus laevis oocytes. NKCC1 RNA (15 ng) was injected on day 2, and WNK4 and SPAK wild type and mutants (10 ng) were injected on day 3. ^{86}Rb uptake was measured on day 5 in an isosmotic solution containing 1 mM ouabain. (B) Expression of WNK4 with full-length SPAK, shortened SPAK (-PAPA box), and OSR1 in NKCC1-injected Xenopus laevis oocytes. Bars represent means ± standard errors of the means (n = 20 oocytes). The experiment was repeated twice with identical results.
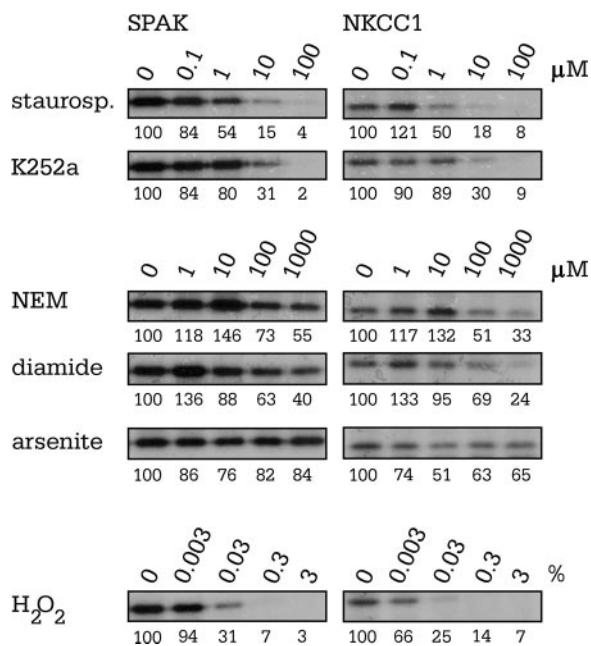
FIG. 7. Pharmacological inhibition of SPAK autophosphorylation. All in vitro phosphorylation reaction mixtures contained identical amounts of SPAK, NKCC1, $MnCl_2$, ATP, $[\gamma\text{-}^{32}P]$ATP, DTT, and Na-HEPES but increasing concentrations of pharmacological agents. Concentrations of staurosporine and K252a ranged from 0.1 to 100 μM. Concentrations of NEM, diamide, and arsenite ranged from 1 μM to 1 mM. Hydrogen peroxide was obtained as a 3% solution. This corresponds to a concentration of ~900 mM H_2O_2. Reactions were loaded on 10% acrylamide gels. Gels were washed, dried, and exposed to autoradiography. The panels are representative of two to three independent experiments.

residues T243 or T247 into alanines greatly impacted kinase activity, as determined through autophosphorylation and transphosphorylation of the N-terminal tail of NKCC1, whereas alanine substitution of T231 and T236 remained silent (Fig. 3). In parallel to these in vitro phosphorylation experiments, we performed functional experiments with the threonine mutants in *Xenopus laevis* oocytes and confirmed the requirement of T243 and T247 for NKCC1 activation (Fig. 6).

Substrate recognition of many protein kinases depends, at least partly, on residues flanking the specific site of substrate phosphorylation (or "P site") with residues N terminal to the P site numbered P−1, P−2, and P−3 and residues C terminal to the P sites numbered P+1, P+2, P+3, etc. (1). In the case of the Ste20p-like protein kinase TAO2, it was shown that its physiological substrates MEK3 and MEK6 both possess hydrophobic residues immediately following the P site (P+1) in both of their two phosphorylation sites (58). For NKCC1, one of the physiological substrates of SPAK, Darman and Forbush have identified the principal P site of shark NKCC1 as T189 (11). Consistent with observations of MEK3 and MEK6, this site is directly followed by a hydrophobic methionine residue. Amino acid sequence alignment of the catalytic domain of mammalian Ste20p-like kinases reveals conservation of a quartet of hydrophobic residues forming a pocket that interacts with the P+1 site. As seen in Fig. 1A, the hydrophobic residues lining the P+1 pocket in SPAK are F244, M251, P253, and L278. Further

analysis of the activation loop of SPAK reveals that residues T243 and T247, newly defined as critical for SPAK activity, are themselves directly followed by hydrophobic residues, phenylalanine following T243 and a proline residue coming after T247, whereas T231 and T236 are followed by nonhydrophobic glycine and arginine residues, respectively. This observation suggests that T243 and T247 might be phosphorylated in a manner similar to the phosphorylation of Ste20p substrates. Interestingly, Vitari et al. identified T243 as a target of WNK1 and WNK4 (54), and both kinases possess the conserved quartet of hydrophobic residues: V383, M390, P392, and M415 for mouse WNK1 and V333, M340, P342, and P365 for mouse WNK4. However, as our in vitro phosphorylation experiments showed that SPAK itself can incorporate phosphates on T243 and T247 (autophosphorylation), whether or not the P+1 pocket is involved is currently unknown. On the basis of the presence of a dimerization region in the regulatory domain of MST1, a Ste20p-like kinase involved in apoptosis, Glantschnig et al. (21) argued that dimerization promotes phosphorylation between individual MST1 molecules. They indeed demonstrated intermolecular phosphorylation by using kinase-active and -inactive forms of MST1. Our yeast two-hybrid data indicate the absence of SPAK-SPAK interaction, making it therefore unlikely that SPAK possesses a dimerization domain. This observation is in agreement with the absence of any multimerization products on Western blots (44). Because of the absence of SPAK-SPAK interaction, we thought it was important to ask whether, in the absence of dimerization, one could see intermolecular phosphorylation. Our experiments clearly indicate that autophosphorylation occurs intramolecularly, as the ability of SPAK to autophosphorylate appears dilution independent (Fig. 4B and C) and as active SPAK is unable to phosphorylate catalytically inactive SPAK (Fig. 4D).

An interesting observation was that Mn^{2+}, but not Mg^{2+}, was very effective as a cofactor in our in vitro phosphorylation experiments. This particular divalent metal ion specificity has been reported for a few kinases (2, 39, 43, 57) and nucleotide binding proteins (56). Whether or not the same specificity exists in vivo remains to be determined. Slightly different conformational changes of the SPAK active site might be generated depending upon the nature of the divalent metal coordinated to the polyphosphate region of the nucleotide. Indeed, X-ray crystallography of CheA showed that the active site of this histidine kinase is greatly influenced by the divalent metal ion bound to the nucleotide, with Mg^{2+} enabling a more extensive conformational change than Mn^{2+} (3). Stronger autophosphorylation with Mn^{2+} in our in vitro experiments might indicate a more open or relaxed conformation of SPAK. In some cases, Mn^{2+} has also been shown to facilitate the use of GTP as a phosphoryl group donor (22). This is clearly not the case with SPAK, where GTP cannot substitute for ATP (Fig. 2). Since Mg^{2+} is more physiologically relevant, it is possible that in vivo, autophosphorylation of the threonines in the activation loop might be minimal, allowing for phosphorylation by other upstream kinases such as WNK1 and/or WNK4.

Experiments performed using internally dialyzed squid giant axons in the late 1970s revealed that Na-K-2Cl cotransport is inhibited by high intracellular Cl^- concentrations. This effect, reproduced in a variety of other cell types, is not related to the ion driving force, since increased intracellular Cl^- concentra-

tions also inhibit Na-K-2Cl cotransport-mediated efflux. Of interest is the demonstration that NKCC1 phosphorylation increases with decreases in Cl^- concentrations (for a review, see reference 46). We examined the Cl sensitivity of both SPAK and OSR1 phosphorylation and found an inhibitory effect in the physiological range (4 to 40 mM). Whether or not the effect of Cl^- concentrations on SPAK autophosphorylation is large enough to account for the exquisite sensitivity of NKCC1 to internal Cl^- concentrations in vivo remains to be determined.

Yeast two-hybrid experiments have previously demonstrated that OSR1, a kinase closely related to SPAK, interacts with the K-Cl cotransporter (KCC3) (44). Immunofluorescence studies with polyclonal antibodies have also demonstrated colocalization of OSR1 and NKCC1 (35). It is therefore not surprising that OSR1, like SPAK, when coexpressed with WNK4 activates NKCC1 in *Xenopus laevis* oocytes. Consistent with these results, our in vitro phosphorylation experiments indicate that OSR1 exhibits many of the same kinetic properties as SPAK. Previous in vivo studies examining OSR1 phosphorylation have shown an increase in kinase activity when the cells were incubated with sorbitol (8). This hyperosmotic activation of OSR1 is consistent with an increase in cotransporter activity under similar conditions, a process we showed to be at least partially related to SPAK (18). Taken together, these results indicate that the shared homology between OSR1 and SPAK is sufficient for either kinase to serve as a modulator of NKCC1 activity.

Over the past 25 years, a variety of inhibitors and activators of both cotransporters have been identified. These pharmacological interventions generally produce opposite effects and therefore are thought to act on the kinases and/or phosphatases which regulate cotransporter activity. Here, we had the possibility of testing the direct effect of several of these agents on both SPAK autophosphorylation and substrate phosphorylation of NKCC1. Staurosporine is a potent inhibitor of the Na-K-2Cl cotransporter (17, 24, 37, 53) and an activator of the K-Cl cotransporter (5, 16, 48). We report here that staurosporine inhibits SPAK activity by ~50% at drug concentrations between 0.1 and 1 μM, consistent with a measured 50% inhibitory concentration of 0.7 μM in avian erythrocytes (33). K252a, another protein kinase inhibitor preventing Na-K-2Cl cotransport stimulation in a variety of cells (40, 42), also inhibited SPAK activity, although requiring slightly higher concentrations than staurosporine. In contrast, arsenite, which stimulates stress-activated protein kinases (27) and MAPKs (32) and markedly activates Na-K-2Cl cotransport in ferret red cells (17), had little effect on SPAK autophosphorylation. This seems to indicate that the arsenite effect in ferret erythrocytes is not directly associated with the kinase that phosphorylates the cotransporter.

We also demonstrated a direct inhibitory effect of hydrogen peroxide on SPAK autophosphorylation as well as transphosphorylation of NKCC1. Hydrogen peroxide (H_2O_2) has been shown to stimulate K-Cl cotransport (4, 6, 41), although the oxidant was believed to act through a phosphatase rather than a volume-sensitive kinase, as calyculin substantially inhibited the H_2O_2 activation (4). Although there are no reports of a H_2O_2 effect on Na-K-2Cl cotransport, tert-butyl hydroperoxide has been shown to have an inhibitory effect on the "regulatory"

kinase (15, 47). Thus, our data showing SPAK inhibition by H_2O_2 are consistent with oxidative reagents inhibiting K-Cl cotransport and activating Na-K-2Cl cotransport. K-Cl cotransport was first defined as a mechanism promoting volume-induced (14) and NEM-induced (29) Cl^--dependent K^+ flux. First, it was proposed that the alkylating reagent reacts with thiol groups located on the transport molecule (for a review, see reference 28). However, in light of the fact that NEM also inhibits Na-K-2Cl cotransport, consensus has moved toward the idea that NEM acts as a protein kinase inhibitor, antagonizing the effect of calyculin A (e.g., see reference 37). The concentration of NEM (1 mM) required to affect K-Cl cotransport in native red cells (29), rabbit KCC1 heterologously expressed in HEK293 cells (20), and Na-K-2Cl cotransport in native red cells (37) is relatively high. We showed that 1 mM NEM minimally affects SPAK autophosphorylation but significantly decreases the level of NKCC1 phosphorylation. This observation suggests that despite SPAK autophosphorylation of the activation loop threonine residues, NEM still prevents kinase-substrate interaction, cotransporter phosphorylation, and, ultimately, functional activation. Interestingly, the sulfhydryl oxidant, diamide, produced similar effects on SPAK autophosphorylation and NKCC1 transphosphorylation, further evidence that the effector sites of these agents lie between SPAK and the cotransporters.

The effect of NEM is intriguing, since it clearly delineates two separate events: SPAK autophosphorylation and kinase phosphorylation of the cotransporter. Data obtained with our deletion mutants (Fig. 3B) also demonstrate that kinase autophosphorylation by itself is not sufficient but that a portion of the regulatory domain proximal to the catalytic domain is necessary for substrate phosphorylation. The fact that WNK1 and WNK4 phosphorylate SPAK on residue S383 (located within this proximal region of the regulatory domain) indicates that access of the substrate to the kinase domain might depend on some conformation changes triggered by phosphorylation of the C terminus.

In summary, our results demonstrate that SPAK and OSR1 are kinases regulated through activation segment phosphorylation. We found that two of the four threonine residues (T243 and T247) within the activation loop were critical for SPAK autophosphorylation, and subsequent substrate phosphorylation and activation of NKCC1. Through mutagenesis studies, we determined that in vitro phosphorylation of these key threonine residues occurs by intramolecular autophosphorylation. We also found that although truncation of the regulatory domain allowed SPAK autophosphorylation, a proximal portion of the regulatory domain (~70 amino acids) was necessary for NKCC1 phosphorylation. Finally, we demonstrate that pharmacological inhibitors of NKCC1, i.e., staurosporine and K252a, directly affect SPAK autophosphorylation and substrate phosphorylation of the cotransporter. Taken together, these results clearly indicate that SPAK (and OSR1) likely represent two of the kinases which phosphorylate and activate NKCC1.

REFERENCES

1. **Adams, J. A.** 2001. Kinetic and catalytic mechanisms of protein kinases. Chem. Rev. **101:**2271–2290.

2. **Bengs, F., A. Scholz, D. Kuhn, and M. Wiese.** 2005. LmxMPK9, a mitogen-activated protein kinase homologue affects flagellar length in *Leishmania mexicana*. Mol. Microbiol. **55:**1606–1615.

3. **Bilwes, A. M., C. M. Quezada, L. R. Croal, B. R. Crane, and M. I. Simon.** 2001. Nucleotide binding by the histidine kinase CheA. Nat. Struct. Biol. **8:**353–360.

4. **Bize, I., and P. B. Dunham.** 1995. H2O2 activates red blood cell K-Cl cotransport via stimulation of a phosphatase. Am. J. Physiol. Cell Physiol. **269:**C849–C855.

5. **Bize, I., and P. B. Dunham.** 1994. Staurosporine, a protein kinase inhibitor, activates K-Cl cotransport in LK sheep erythrocytes. Am. J. Physiol. Cell Physiol. **266:**C759–C770.

6. **Bogdanova, A. Y., and M. Nikinmaa.** 2001. Reactive oxygen species regulate oxygen-sensitive potassium flux in rainbow trout erythrocytes. J. Gen. Physiol. **117:**181–190.

7. **Callow, M. G., S. Zozulya, M. L. Gishizky, B. Jallal, and T. Smeal.** 2005. PAK4 mediates morphological changes through the regulation of GEF-H1. J. Cell Sci. **118:**1861–1872.

8. **Chen, W., M. Yazicioglu, and M. H. Cobb.** 2004. Characterization of OSR1, a member of the mammalian Ste20p/germinal center kinase subfamily. J. Biol. Chem. **279:**11129–11136.

9. **Cossins, A. R., Y. R. Weaver, G. Lykkeboe, and O. B. Nielsen.** 1994. Role of protein phosphorylation in control of K flux pathways of trout red blood cells. Am. J. Physiol. Cell Physiol. **267:**C1641–C1650.

10. **Dan, I., N. M. Watanabe, and A. Kusumi.** 2001. The Ste20 group kinases as regulators of MAP kinase cascades. Trends Cell. Biol. **11:**220–230.

11. **Darman, R. B., and B. Forbush.** 2002. A regulatory locus of phosphorylation in the N terminus of the Na-K-Cl cotransporter, NKCC1. J. Biol. Chem. **277:**37542–37550.

12. **Denton, J., K. Nehrke, X. Yin, R. Morrison, and K. Strange.** 2005. GCK-3, a newly identified Ste20 kinase, binds to and regulates the activity of a cell cycle-dependent ClC anion channel. J. Gen. Physiol. **125:**113–125.

13. **Dowd, B. F., and B. Forbush.** 2003. PASK (proline-alanine-rich STE20-related kinase), a regulatory kinase of the Na-K-Cl cotransporter (NKCC1). J. Biol. Chem. **278:**27347–27353.

14. **Dunham, P. B., and J. C. Ellory.** 1981. Passive potassium transport in low potassium sheep red cells: dependence upon cell volume and chloride. J. Physiol. (London) **318:**511–530.

15. **Elliott, S. J., and W. P. Schilling.** 1992. Oxidant stress alters Na+ pump and Na(+)-K(+)-Cl- cotransporter activities in vascular endothelial cells. Am. J. Physiol. **263:**H96–H102.

16. **Flatman, P. W., N. C. Adragna, and P. K. Lauf.** 1996. Role of protein kinases in regulating sheep erythrocyte K-Cl cotransport. Am. J. Physiol. Cell Physiol. **271:**C255–C263.

17. **Flatman, P. W., and J. Creanor.** 1999. Stimulation of Na$^+$-K$^+$-2Cl$^-$ cotransport by arsenite in ferret erythrocytes. J. Physiol. **519:**143–152.

18. **Gagnon, K. B., R. England, and E. Delpire.** 2006. Volume sensitivity of cation-chloride cotransporters is modulated by the interaction of two kinases: SPAK and WNK4. Am. J. Physiol. Cell Physiol. **290:**134–142.

19. **Gamba, G.** 2005. Molecular physiology and pathophysiology of electroneutral cation-chloride cotransporters. Physiol. Rev. **85:**423–493.

20. **Gillen, C. M., S. Brill, J. A. Payne, and B. I. Forbush.** 1996. Molecular cloning and functional expression of the K-Cl cotransporter from rabbit, rat, and human. A new member of the cation-chloride cotransporter family. J. Biol. Chem. **271:**16237–16244.

21. **Glantschnig, H., G. A. Rodan, and A. A. Reszka.** 2002. Mapping of MST1 kinase sites of phosphorylation. Activation and autophosphorylation. J. Biol. Chem. **277:**42987–42996.

22. **Graves, P. R., C. Bartleson, A. Biorn, and M. Pete.** 1999. Substrate and inhibitor recognition of protein kinases: what is known about the catalytic subunit of phosphorylase kinase? Pharmacol. Ther. **82:**143–155.

23. **Graves, J. D., Y. Gotoh, K. E. Draves, D. Ambrose, D. K. Han, M. Wright, J. Chernoff, E. A. Clark, and E. G. Krebs.** 1998. Caspase-mediated activation and induction of apoptosis by the mammalian Ste20-like kinase Mst1. EMBO J. **17:**2224–2234.

24. **Homma, T., K. D. Burns, and R. C. Harris.** 1990. Agonist stimulation of Na$^+$/K$^+$/Cl$^-$ cotransport in rat glomerular mesangial cells. Evidence for protein kinase C-dependent and Ca2+/calmodulin-dependent pathways. J. Biol. Chem. **265:**17613–17620.

25. **Hubbard, S. R.** 1997. Crystal structure of the activated insulin receptor tyrosine kinase in complex with peptide substrate and ATP analog. EMBO J. **16:**5572–5581.

26. **Johnston, A. M., G. Naselli, L. J. Gonez, R. M. Martin, L. C. Harrison, and H. J. Deaizpurua.** 2000. SPAK, a Ste20/SPS1-related kinase that activates the p38 pathway. Oncogene **19:**4290–4297.

27. **Kyriakis, J. M., P. Banerjee, E. Nikolakaki, T. Dai, E. A. Rubie, M. F. Ahmad, J. Avruch, and J. R. Woodgett.** 1994. The stress-activated protein kinase subfamily of c-Jun kinases. Nature **369:**156–160.

28. **Lauf, P. K.** 1985. K$^+$Cl$^-$ cotransport: sulfhydrals, divalent cations, and the mechanism of volume activation in a red cell. J. Membr. Biol. **88:**1–13.

29. **Lauf, P. K., and B. E. Theg.** 1980. A chloride dependent K$^+$ flux induced by N-ethylmaleimide in genetically low K$^+$ sheep and goat erythrocytes. Biochem. Biophys. Res. Commun. **70:**221–242.

30. **Li, Y., J. Hu, R. Vita, B. Sun, H. Tabata, and A. Altman.** 2004. SPAK kinase is a substrate and target of PKCtheta in T-cell receptor-induced AP-1 activation pathway. EMBO J. **23:**1112–1122.

31. **Lin, J. L., H. C. Chen, H. I. Fang, D. Robinson, H. J. Kung, and H. M. Shih.** 2001. MST4, a new Ste20-related kinase that mediates cell growth and transformation via modulating ERK pathway. Oncogene **20:**6559–6569.

32. **Ludwig, S., A. Hoffmeyer, M. Goebeler, K. Kilian, H. Hafner, B. Neufeld, J. Han, and U. R. Rapp.** 1998. The stress inducer arsenite activates mitogen-activated protein kinases extracellular signal-regulated kinases 1 and 2 via a MAPK kinase 6/p38-dependent pathway. J. Biol. Chem. **273:**1917–1922.

33. **Lytle, C.** 1997. Activation of the avian erythrocyte Na-K-Cl cotransport protein by cell shrinkage, cAMP, fluoride, and calyculin-A involves phosphorylation at common sites. J. Biol. Chem. **272:**15069–15077.

34. **Lytle, C.** 1998. A volume-sensitive protein kinase regulates the Na-K-2Cl cotransporter in duck red blood cells. Am. J. Physiol. Cell Physiol. **274:**C1002–C1010.

35. **Marshall, W. S., C. G. Ossum, and E. K. Hoffmann.** 2005. Hypotonic shock mediation by p38 MAPK, JNK, PKC, FAK, OSR1 and SPAK in osmosensing chloride secreting cells of killifish opercular epithelium. J. Exp. Biol. **208:**1063–1077.

36. **Miao, N., B. Fung, R. Sanchez, J. Lydon, D. Barker, and K. Pang.** 2000. Isolation and expression of PASK, a serine/threonine kinase during rat embryonic development, with special emphasis on the pancreas. J. Histochem. Cytochem. **48:**1391–1400.

37. **Muzyamba, M. C., A. R. Cossins, and J. S. Gibson.** 1999. Regulation of Na$^+$-K$^+$-2Cl$^-$ cotransport in turkey red cells: the role of oxygen tension and protein phosphorylation. J. Physiol. (London) **517:**421–429.

38. **Nolen, B., S. Taylor, and G. Ghosh.** 2004. Regulation of protein kinases; controlling activity through activation segment conformation. Mol. Cell **15:**661–675.

39. **Novakova, L., L. Saskova, P. Pallova, J. Janecek, J. Novotna, A. Ulrych, J. Echenique, M. C. Trombe, and P. Branny.** 2005. Characterization of a eukaryotic type serine/threonine protein kinase and protein phosphatase of *Streptococcus pneumoniae* and identification of kinase substrates. FEBS J. **272:**1243–1254.

40. **O'Donnell, M. E., A. Martinez, and D. Sun.** 1995. Endothelial Na-K-Cl cotransport regulation by tonicity and hormones: phosphorylation of cotransport protein. Am. J. Physiol. Cell Physiol. **269:**C1513–C1523.

41. **Olivieri, O., M. Bonollo, S. Friso, D. Girelli, R. Corrocher, and L. Vettore.** 1993. Activation of K$^+$/Cl$^-$ cotransport in human erythrocytes exposed to oxidative agents. Biochim. Biophys. Acta **1176:**37–42.

42. **Palfrey, H. C., and E. B. Pewitt.** 1993. The ATP and Mg2$^+$ dependence of Na(+)-K(+)-2Cl$^-$ cotransport reflects a requirement for protein phosphorylation: studies using calyculin A. Pflueg. Archiv. **425:**321–328.

43. **Petrickova, K., P. Tichy, and M. Petricek.** 2000. Cloning and characterization of the *pknA* gene from *Streptomyces coelicolor* A3(2), coding for the Mn2$^+$ dependent protein Ser/Thr kinase. Biochem. Biophys. Res. Commun. **279:**942–948.

44. **Piechotta, K., N. J. Garbarini, R. England, and E. Delpire.** 2003. Characterization of the interaction of the stress kinase SPAK with the Na$^+$-K$^+$-2Cl$^-$ cotransporter in the nervous system: evidence for a scaffolding role of the kinase. J. Biol. Chem. **278:**52848–52856.

45. **Piechotta, K., J. Lu, and E. Delpire.** 2002. Cation-chloride cotransporters interact with the stress-related kinases SPAK and OSR1. J. Biol. Chem. **277:**50812–50819.

46. **Russell, J. M.** 2000. Sodium-potassium-chloride cotransport. Physiol. Rev. **80:**211–276.

47. **Sen, C. K., I. Kolosova, O. Hanninen, and S. N. Orlov.** 1995. Inward potassium transport systems in skeletal muscle derived cells are highly sensitive to oxidant exposure. Free Radic. Biol. Med. **18:**795–800.

48. **Shen, M. R., C. Y. Chou, K. F. Hsu, Y. M. Hsu, W. T. Chiu, M. J. Tang, S. L. Alper, and J. C. Ellory.** 2003. KCl cotransport is an important modulator of human cervical cancer growth and invasion. J. Biol. Chem. **278:**39941–39950.

49. **Strange, K., T. D. Singer, R. Morrison, and E. Delpire.** 2000. Dependence of KCC2 K-Cl cotransporter activity on a conserved carboxy terminus tyrosine residue. Am. J. Physiol. Cell Physiol. **279:**C860–C867.

50. **Tamari, M., Y. Daigo, and Y. Nakamura.** 1999. Isolation and characterization of a novel serine threonine kinase gene on chromosome 3p22-21.3. J. Hum. Genet. **44:**116–120.

51. **Tsutsumi, M., M. K. Skinner, and E. Sanders-Bush.** 1989. Transferrin gene expression and synthesis by cultured choroid plexus epithelial cells. J. Biol. Chem. **264:**9626–9631.

52. **Ushiro, H., T. Tsutsumi, K. Suzuki, T. Kayahara, and K. Nakano.** 1998. Molecular cloning and characterization of a novel Ste20-related protein kinase enriched in neurons and transporting epithelia. Arch. Biochem. Biophys. **355:**233–240.

53. **Vigne, P., A. Lopez Farre, and C. Frelin.** 1994. Na(+)-K(+)-Cl− cotransporter of brain capillary endothelial cells. Properties and regulation by endothelins, hyperosmolar solutions, calyculin A, and interleukin-1. J. Biol. Chem. **269:**19925–19930.

54. **Vitari, A. C., M. Deak, N. A. Morrice, and D. R. Alessi.** 2005. The WNK1 and WNK4 protein kinases that are mutated in Gordon's hypertension syndrome, phosphorylate and active SPAK and OSR1 protein kinases. Biochem. J. **391:**17–24.

55. **Wilson, F. H., K. T. Kahle, E. Sabath, M. D. Lalioti, A. K. Rapson, R. S. Hoover, S. C. Hebert, G. Gamba, and R. P. Lifton.** 2003. Molecular pathogenesis of inherited hypertension with hyperkalemia: the Na-Cl cotransporter is inhibited by wild-type but not mutant WNK4. Proc. Natl. Acad. Sci. USA **100:**680–684.

56. **Wu, C. C., T. Y. Hsu, and J. Y. Chen.** 2005. Characterization of three essential residues in the conserved ATP-binding region of Epstein-Barr virus thymidine kinase. Biochemistry **44:**4785–4793.

57. **Yu, K. T., N. Khalaf, and M. P. Czech.** 1987. Insulin stimulates a novel Mn^{2+}-dependent cytosolic serine kinase in rat adipocytes. J. Biol. Chem. **262:**16677–16685.

58. **Zhou, T., M. Raman, Y. Gao, S. C. Earnest, Z., M. Machius, M. H. Cobb, and E. J. Goldsmith.** 2004. Crystal structure of the TAO2 kinase domain: activation and specificity of a Ste20p MAP3K. Structure **12:**1891–1900.